2 July 1999

ELSEVIER

Chemical Physics Letters 307 (1999) 131–138

CHEMICAL PHYSICS LETTERS

www.elsevier.nl/locate/cplett

Cavity-enhanced absorption spectroscopy of the 1.5 μm band system of jet-cooled ammonia

Giel Berden *, Rudy Peeters, Gerard Meijer

Department of Molecular and Laser Physics, University of Nijmegen, Toernooiveld, 6525 ED Nijmegen, The Netherlands

Received 15 April 1999

Abstract

Absorption spectra of rotationally cold ammonia ($^{14}NH_3$) molecules have been recorded in the 6400–6630 cm^{-1} region, using the cavity-enhanced absorption technique in combination with a slit-nozzle expansion. Two perpendicular rovibrational bands have been identified: the $\nu_1 + \nu_3$ band at 6609 cm^{-1}, and a 'new' band at 6557 cm^{-1} which is tentatively assigned to a transition into the $|l| = 2$ component of the $\nu_1 + 2\nu_4$ state.

1. Introduction

The availability of compact and cheap near-infrared tunable diode lasers has led to the development of simple and inexpensive spectroscopic systems for detection and monitoring of molecules in the atmosphere and in industrial processes [1]. For ammonia, several diode laser-based detection and monitoring systems have been developed which use spectral lines from the near-infrared bands around 1.5 μm [2–9], a spectral region which contains various weak overtone and combination bands.

Spectroscopically, there is not much known about the bands of ammonia in the 1.5 μm region. The first spectrum showing (not well-resolved) rotational structure has been reported by Unger in 1933 [10]. A spectrum at a resolution of 0.2 cm^{-1} was recorded and analyzed by Benedict and Plyler in 1957 [11]. They reported the combination band $\nu_1 + \nu_3$ at 6608.71 cm^{-1}, the overtone band $2\nu_3$ ($|l| = 2$) at 6850.2 cm^{-1}, and tentatively assigned the $\nu_1 + 2\nu_4$ to be around 6700 cm^{-1}. The development of single-frequency 1.5 μm diode lasers for optical communication provided lists of high-resolution absorption lines of ammonia [2,12,13]. As these lines were mainly used to test the frequency stabilization of the laser, or for locking the laser to an absorption line, however, no attempt for a rovibrational assignment was made.

Lundsberg-Nielsen et al. [14] reported the first complete high-resolution absorption spectrum of ammonia covering the 6400–6900 cm^{-1} region. The spectrum obtained at a resolution of 0.005 cm^{-1} using a Fourier transform spectrometer, is very complex with many blended lines. A total of 1710 lines were observed, and 381 rotational–vibrational transitions have been assigned to the combination band $\nu_1 + \nu_3$ (at 6609.6 cm^{-1}) and the overtone band $2\nu_3$ (at 6794 cm^{-1}). The assignments were performed by calculating ground state combination dif-

* Corresponding author. Fax: +31 24 3653311; e-mail: giel@sci.kun.nl

0009-2614/99/$ - see front matter
PII: S0009-2614(99)00504-7

ferences (GSCDs) using accurate ground state energy levels reported by Urban et al. [15].

A complete analysis of the rovibrational bands of ammonia in the 1.5 μm region is a formidable task. Many vibrational bands are expected in this region: the $2\nu_1$, $2\nu_3$, $\nu_1+\nu_3$, $\nu_1+2\nu_4$, $\nu_3+2\nu_4$, $4\nu_4$, $\nu_1+4\nu_2$, $4\nu_2+\nu_3$, $4\nu_2+2\nu_4$, and so on. Perturbations are present due to rather complicated interactions involving many of these overtone and combination vibrational bands. Local perturbations give rise to strong frequency and intensity changes.

In order to obtain some feeling for these perturbations, it is informative to look at the absorption bands of ammonia around 3 μm [16,17]. In this region the fundamentals ν_1 and ν_3 are located, but also the $2\nu_4$ and the $4\nu_2$ overtones and the $2\nu_2+\nu_4$ combination band. Recently, some 2110 lines from the ν_1, ν_3, and $2\nu_4$ bands were assigned out of which 1832 line positions were fitted using an effective rotation–inversion Hamiltonian [17]. However, there are still some discrepancies, which can only be removed if more information becomes available on the $4\nu_2$ and $2\nu_2+\nu_4$ bands [17].

In the case of the 1.5 μm band system, the GSCDs analysis has led to the assignment of only 22% of the rovibrational transitions [14]. Even in the region of the vibrational origin of the $\nu_1+\nu_3$ band many lines are unassigned. In order to aid in the further analysis, we decided to focus on the rotational states with low rotational quantum numbers by recording the absorption spectrum of ammonia in a supersonic molecular jet. Due to rotational cooling the spectra are strongly simplified, and an assignment of the lowest rotational–vibrational transitions can be made.

Since the concentration of ammonia in the jet should be rather low in order to obtain sufficient rotational cooling [18], direct absorption laser spectroscopy in a jet requires a sensitive detection scheme. In this study we use the cavity-enhanced absorption (CEA) technique [8] in combination with a slit-nozzle expansion. With this method the effective absorption path length is about 100 m, and an absorption spectrum can be measured to which only the $J''=0$ and the $J''=1$ levels contribute. This spectrum can easily be assigned. By slightly increasing the ammonia concentration, the rotational temperature can be increased, leading to more transitions in the absorption spectrum. In this way we have assigned 18 transitions to the $\nu_1+\nu_3$ band. Additionally, a new vibrational band is identified, whose origin is 52 cm^{-1} red-shifted with respect to the vibrational origin of the $\nu_1+\nu_3$ band.

2. Experiment

A scheme of the experimental arrangement is shown in Fig. 1. A planar jet is formed by expanding ammonia strongly diluted in argon through a 40×0.03 mm slit nozzle. In order to measure spectra of ammonia with different (but low) rotational temperatures, the amount of ammonia is varied. The vacuum chamber is evacuated by a 1200 m^3/h rootspump (Edwards EH1200) backed by a 180 m^3/h rotary pump (Leybold SV180). At a stagnation pressure of 1 bar the background pressure reaches 1 mbar.

The rotationally resolved absorption spectra of ammonia in the jet are measured by using the CEA technique. This technique has been described in detail before [8], and only a short description is given here. Light of a rapidly scanning cw diode laser is coupled into a non-confocal optical cavity. The cavity axis is along the long axis of the slit nozzle, intersecting the jet a few millimeters downstream from the orifice. The time-integrated intensity of the light leaking out of the cavity is measured as a function of the wavelength. From a plot of the inverse of this intensity versus wavelength, the direct absorption spectrum is obtained.

As a light source we have used a cw diode laser (New Focus model 6262) which is tunable in the 6270–6630 cm^{-1} region with 5 mW maximum power. The specified bandwidth is <5 MHz. The laser has an external cavity and can be scanned mode-hop free over 1 cm^{-1} by piezo tuning the end mirror. A different scan region can be selected by adjusting the end mirror with a pico-motor.

The non-confocal optical cavity is formed by two highly reflecting ($R\approx 0.9995$) plano-concave mirrors with a radius of curvature $r=-1$ m. The distance between the mirrors d is 8.5 cm, and the mirrors can be aligned independently. The light that leaks out of the cavity is detected with a photodiode (New Focus Nirvana 2017). The signal is displayed on a digital oscilloscope (Yokogawa DL4200,

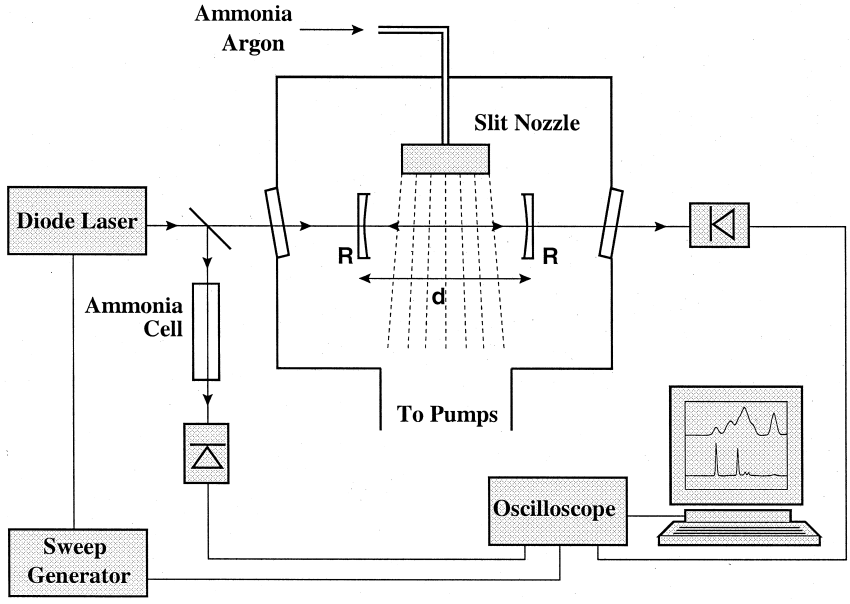

Fig. 1. Experimental arrangement.

10 bits, 300 MHz). To record wavelength spectra, the oscilloscope is used in the *x-y* mode, with the horizontal axis being proportional to the scanning voltage of the diode laser, which in turn is proportional to the wavelength. The laser is scanned over 1 cm^{-1} at a rate of 30 Hz.

A single laser scan provides an absorption spectrum in which the mode structure of the optical cavity is visible (see, e.g., Fig. 1 of Ref. [8]). As has been explained in Ref. [8] the scan rate of the laser should be chosen such that each wavelength is in resonance with a cavity mode equally long and sufficiently long. Since the optical cavity is (mechanically) unstable, the mode spectrum of this cavity 'jitters'. Therefore, summation over several scans (typically 4000) provides a method to sample each wavelength with an equal probability. The remaining 'noise' in the spectra is mainly due to residual mode structure of the cavity.

Since the diode laser is scanned typically over 1 cm^{-1}, wavelength calibration using another molecular absorption spectrum as a reference is difficult and tedious. Therefore, we use the reported wavelengths of ammonia from Lundsberg–Nielsen et al. [14], who have calibrated their Fourier transform spectra against the absorption spectra of C_2H_2. Experimentally, we record a single-pass absorption spectrum of ammonia in a cell at room temperature simultaneously with the CEA spectrum of ammonia in the jet.

3. Results and discussion

The symmetries of the fundamentals of ammonia are [1] ν_1 (A), ν_2 (A), ν_3 (E), and ν_4 (E). Bands from the vibrational ground state towards an E state are perpendicular, whereas those towards an A state are parallel.

In the 3 μm band system, the strongest bands are the ν_1, the ν_3, and the $2\nu_4$, with bandstrengths of 23.6, 11.8, and 2.8 cm^{-2}/atm at 296 K, respectively [17]. Therefore, the strongest bands expected in the 1.5 μm region are the $2\nu_1$, $2\nu_3$, $\nu_1+\nu_3$, $\nu_1+2\nu_4$, and $\nu_3+2\nu_4$ bands.

[1] This 'short' description more or less 'includes' the tunneling of ammonia. In the molecular symmetry group D_{3h}, the symmetries of the fundamentals of ammonia are ν_1 (A_1'), ν_{inv} (A_2''), ν_3 (E′), and ν_4 (E′) [19]. Furthermore, note that $n\nu_2^s = 2n\nu_{inv}$ and $n\nu_2^a = (2n+1)\nu_{inv}$. Rotational transitions from the vibrational ground state towards an E′ state are perpendicular, and transitions towards an A_2'' state are parallel.

The vibrational origin of the $\nu_1 + \nu_3$ band is reported at 6609.6 cm^{-1} and the origin of the $2\nu_3$ ($l = 0$) at 6794 cm^{-1} [14]. Our diode laser can only cover the 6270–6630 cm^{-1} region. Therefore, rovibrational transitions of the $2\nu_3$ band are not accessible, and only about 60% of the rovibrational transitions of the $\nu_1 + \nu_3$ band can be recorded with the present arrangement.

Two spectra have been recorded. The 'coldest' spectrum, with an estimated rotational temperature of about 10 K, contains only 10 rotational transitions. The 'warmer' spectrum, with an estimated rotational temperature of about 30 K, shows 29 spectral lines.

3.1. The $\nu_1 + \nu_3$ band

Eight of the measured lines have been previously assigned as belonging to the perpendicular $\nu_1 + \nu_3$ band [14]. Because the rotationally cold spectra contain only rotational transitions originating from $J'' = 0,1$ (the 'coldest' spectrum) and $J'' = 0,1,2$ (the 'warmer' spectrum), a complete assignment of the

Table 1
Observed transitions of $^{14}NH_3$ in the 6400–6630 cm^{-1} region. Line numbers correspond to the numbers in the paper of Lundsberg–Nielsen et al. [14], · (∘) indicates that the present rotational assignment is (not) in agreement with their assignment. In the column 'Remarks', 'c' indicates that the transition is also observed in the 'coldest' spectrum. Furthermore, √ indicates that the assignment is verified with GSCD using transitions only from this table. When in parenthesis, the assignment is verified with GSCD using lines from Tables II and III of Ref. [14]. The upper state energies are calculated using the ground state energy levels from Ref. [15]; the non-existing ($J'' = 0$, $K'' = 0$, s) level in the ground state is taken at 0 cm^{-1}.

Rotational assignment							Observed fr. (cm^{-1})	Line no.	Remarks		Upper state energy (cm^{-1})
J''	K''	inv''	J'	K'	l'	inv'					
						$\nu_1 + \nu_3$					
2	0	a	1	1	+1	a	6564.856	441 ·		√	6625.269
2	1	s	1	0		s	6572.848	474		√	6628.787
2	1	a	1	0		a	6572.947	476 ∘		√	6629.656
2	2	s	1	1	−1	s	6580.600	516 ·	c		6625.396
2	2	a	1	1	−1	a	6580.721	518 ·	c		6626.308
1	1	s	0	0		s	6592.644	579	c		6608.817
1	1	a	0	0		a	6592.784	580	c		6609.747
2	1	s	2	2	+1	s	6596.343	602 ·		(√)	6652.282
2	1	a	2	2	+1	a	6596.438	–		(√)	6653.147
1	0	s	1	1	+1	s	6604.722	656	c		6624.612
2	0	a	2	1	+1	a	6605.097	658	c		6665.510
1	1	s	1	0		s	6612.615	701	c	√	6628.788
1	1	a	1	0		a	6612.695	–	c	√	6629.658
2	1	a	2	0		a	6612.723	–		(√)	6669.432
2	1	s	2	0		s	6612.734	–		(√)	6668.673
2	2	s	2	1	−1	s	6620.571	758 ·		(√)	6665.367
2	2	a	2	1	−1	a	6620.578	759 ·		(√)	6666.165
0	0	a	1	1	+1	a	6624.476	788 ·	c	√	6625.269
						$\nu_1 + 2\nu_4$					
1	1	s	0	0		s	6540.244	339			6556.417
1	1	a	0	0		a	6540.965	342			6557.928
1	0	s	1	1	−2	s	6547.941	361			6567.831
1	1	s	1	0		s	6560.819	416		(√)	6576.992
1	1	a	1	0		a	6561.263	419		(√)	6578.226
0	0	a	1	1	−2	a	6568.463	454	c	(√)	6569.256
1	1	s	2	2	−2	s	6575.074	488		(√)	6591.247
1	1	a	2	2	−2	a	6575.713	492		(√)	6592.676
1	0	s	2	1	−2	s	6589.062	559		(√)	6608.952

jet-cooled $\nu_1 + \nu_3$ spectrum can easily be made. The selection rules are $s \leftarrow s$, $a \leftarrow a$, and $\Delta K = \pm 1$ transitions go to the $l = \pm 1$ Coriolis component [2] [19]. The results are shown in Table 1.

This assignment is verified by calculating the GSCDs using the ground state energy levels reported by Urban et al. [15]. Considering only the transitions measured in the present study, six assignments could be verified. Transitions towards the ($J' = 0$, $K' = 0$) level, the ($J' = 1$, $K' = 1$, $l = -1$) level, the ($J' =$ odd, $K' = 1$, $l = +1$, s) levels, and the ($J' =$ even, $K' = 1$, $l = +1$, a) levels are 'unique', and cannot be verified by GSCDs. The other assignments could be verified by making use of the long list of spectral lines reported in the paper of Lundsberg–Nielsen et al. [14]; actually, in our single-pass absorption spectrum of room temperature ammonia a lot more (weak) transitions are visible than listed in Ref. [14].

Fig. 2 displays the spectral region containing the ${}^{P}Q_1$ branch (transitions are labeled ${}^{\Delta K}\Delta J_K(J)$). The lower panel contains three CEA jet-spectra obtained by expanding different amounts of ammonia in 1 bar argon. The ammonia concentration increases from spectrum I to III. The absorption coefficient κ is expressed in units of $(1 - R)/d_a$. Since the reflection coefficient of the mirrors R is approximately 0.9995, and the effective distance d_a over which ammonia absorbs is about 5 cm, the units of absorption are roughly 1×10^{-4} cm^{-1}.

The upper panel of Fig. 2 shows the corresponding room temperature single-pass absorption spectrum of 3 mbar ammonia. The linewidth of the features in this spectrum is 0.02 cm^{-1} (FWHM) and is dominated by Doppler broadening. Jet-spectrum I (the aforementioned 'coldest' spectrum) contains two strong narrow lines with a width of 0.006 cm^{-1}, determined by the residual Doppler broadening in the jet. These lines are assigned to the ${}^{P}Q_1(1)$ transitions of the two inversion components a and s. Jet-spectrum III (the aforementioned 'warmer' spectrum) contains two extra narrow lines, which are assigned to the ${}^{P}Q_1(2)$ transitions. Additionally, there are several broad features in this spectrum which match very well to the room temperature spectrum and are due to thermalized background ammonia in the cavity.

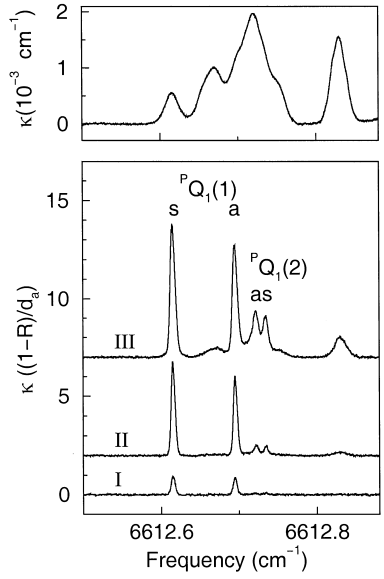

Fig. 2. Part of the $\nu_1 + \nu_3$ spectrum containing the ${}^{P}Q_1$ branch. The lower panel shows the CEA spectra of ammonia in a jet obtained by seeding different amounts of ammonia in argon. The ammonia concentration increases from spectrum I to III. The absorption coefficient κ is expressed in units of $(1 - R)/d_a$ which is about 1×10^{-4} cm^{-1} (see text for further details). The spectra II and III have been given an offset for clarity. The upper panel shows the corresponding part of the single pass absorption spectrum of 3 mbar ammonia at room temperature.

Although a complete analysis of the $\nu_1 + \nu_3$ band is beyond the scope of the present study, we have fitted the excited state energy levels deduced from the observed transitions in the jet spectrum to a simple Hamiltonian in order to obtain more insight in the rotational structure of this state. For comparison, we have fitted the *same* energy levels of the ν_3 state [17] and the $\nu_2 + \nu_3$ state [21] as well. The simple Hamiltonian used is

$$H = B_v J(J+1) + (C_v - B_v) K^2 - 2C_v \zeta_v lK, \quad (1)$$

[2] As a matter of fact, the Coriolis interaction is given by $-2C\zeta lk$, in which k is the signed quantum number of the component of angular momentum along the top axis, i.e. $K = |k|$. Often, the pairs of Coriolis components are classified as $(+l)$ and $(-l)$ [19,20]. For example, the degenerate $l = +1$, $k = -1$ and $l = -1$, $k = +1$ levels are labeled as $K = 1, (-l)$. For simplicity, we write $-2C\zeta lK$ for the Coriolis interaction. The aforementioned degenerate levels are then labeled as $K = 1$, $l = -1$.

with ζ_v the Coriolis coupling constant. The results are presented in Table 2. The molecular constants in this table are given without an error, in order to emphasize that they do not reflect the 'real' constants since they are determined by the very small data set and since perturbations are neglected. The quality of the fit is represented by the value of χ^2 which we have defined as the sum of the squared differences between the observed and calculated energies. The upper levels of the $^{R}Q_0(1)^s$ and $^{R}Q_0(2)^a$ transitions are not included in the fit since their observed minus calculated values are very large (0.2 and 0.4 cm^{-1}, respectively). As a consequence these levels do *not* contribute to the value of χ^2. These local deviations together with a comparison of the χ^2 values of the $\nu_1+\nu_3$ state with those of the ν_3 and $\nu_2+\nu_3$ states, clearly indicate the existence of perturbations in the lowest rotational levels of the $\nu_1+\nu_3$ state.

Comparing the values of the molecular constants of the ν_3, $\nu_2+\nu_3$, and $\nu_1+\nu_3$ states, it is seen that they are reasonable similar. It is interesting to note that the small values of $\Delta B = B'-B''$ for the $\nu_1+\nu_3$ band (0.04 cm^{-1} for the *s* component and 0.01 cm^{-1} for the *a* component) are responsible for the unresolved *Q* branches in the room temperature spectrum (see Fig. 2). This of course complicates a GSCDs analysis of this spectrum [14].

3.2. The $\nu_1+2\nu_4$ band

After the assignment of the $\nu_1+\nu_3$ transitions in the jet-spectra, there were 10 transitions left. Nine of them belong to a perpendicular band, which is about three times weaker than the $\nu_1+\nu_3$ band and which is 52 cm^{-1} red-shifted with respect to the $\nu_1+\nu_3$ band.

Since the band is perpendicular, the symmetry of the excited vibrational state must contain *E* symmetry. Therefore, this band can be an overtone of the ν_3 or ν_4, or a combination band containing ν_3 and/or ν_4. If we just look at the band strengths and the vibrational origins of the ν_1, ν_3, and $2\nu_4$ in the 3 μm region [17], it is concluded that the $\nu_1+2\nu_4$ is a promising candidate for the assignment of the observed band. Since the jet spectrum contains only 9 lines (and a 'complete' band has been observed), they all originate from the $J''=0$ and $J''=1$ levels in the ground state. Comparing the spacings of the rotational transitions of this band with those of the perpendicular bands observed at 3 μm [17], it is evident that the spacings resemble those of the $|l|=2$

Table 2
Comparison of the molecular constants (all in cm^{-1} except ζ which is dimensionless) of the $\nu_1+\nu_3$ state with those of the ν_3 and the $\nu_2+\nu_3$ states, and of the $|l|=2$ component of the $\nu_1+2\nu_4$ state with those of the $2\nu_4$ and $\nu_2+2\nu_4$ states. The number of transitions in each fit (#*N*) is determined by the observed transitions of the $\nu_1+\nu_3$ and $\nu_1+2\nu_4$ bands in the jet spectra (Table 1). χ^2 (in 10^{-6} $(cm^{-1})^2$) is defined here as the sum of the squared differences between the observed and calculated energies. See text for further details. Using the lower state energies of the observed transitions, the ground state constants are $B''=9.943$ cm^{-1}, $C''=6.228$ cm^{-1} for the *s* component, and $B''=9.937$ cm^{-1}, $C''=6.230$ cm^{-1} for the *a* component.

	$(\nu_3)^s$	$(\nu_2+\nu_3)^s$	$(\nu_1+\nu_3)^s$	$(2\nu_4)^s$	$(\nu_2+2\nu_4)^s$	$(\nu_1+2\nu_4)^s$
B'	9.76	9.79	9.98	10.40	10.54	10.28
C'	6.23	6.12	6.13	6.09	5.86	6.01
ζ	0.047	0.037	0.050	−0.225	−0.192	−0.203
ν_0	3443.63	4416.92	6608.81	3240.17	4135.95	6556.42
#*N*	6	6	6	5	5	5
χ^2	31.5	42.6	1953.4	157.5	559.4	84.1
	$(\nu_3)^a$	$(\nu_2+\nu_3)^a$	$(\nu_1+\nu_3)^a$	$(2\nu_4)^a$	$(\nu_2+2\nu_4)^a$	$(\nu_1+2\nu_4)^a$
B'	9.76	9.70	9.95	10.48	10.28	10.15
C'	6.23	6.16	6.18	6.14	6.11	6.05
ζ	0.046	0.040	0.043	−0.230	−0.229	−0.201
ν_0	3443.99	4435.44	6609.72	3241.60	4193.14	6557.93
#*N*	8	8	8	4	4	4
χ^2	36.9	143.2	3687.5	–	–	–

component of the $2\nu_4$ band. This supports the assignment of the observed band to the $|l| = 2$ component of the $\nu_1 + 2\nu_4$ band, which is of exactly the same symmetry. Now an assignment can easily be made. The selection rules are $s \leftarrow s$, $a \leftarrow a$, and $\Delta K = \pm 1$ transitions go to the $l = \mp 2$ Coriolis component [19,20]. The results are shown in Table 1.

Again we have fitted the excited state energies to the simple Hamiltonian given in Eq. (1). For comparison, the *same* energy levels of the $|l| = 2$ component of the $2\nu_4$ [17] and the $\nu_2 + 2\nu_4$ [21] states have been fitted as well. The results are presented in Table 2. It is seen that the molecular constants of the three states containing $2\nu_4$ are reasonable similar (and different from those containing ν_3), which supports the assignment of the observed band to the $\nu_1 + 2\nu_4$ band.

3.3. Alternative vibrational assignment

Two perpendicular bands of ammonia have been observed in the jet and have been assigned to the $\nu_1 + \nu_3$ band and to the $\nu_1 + 2\nu_4$ band ($|l| = 2$ component). No band origins have been observed at lower frequency, but it has to be noted that bands which are 20 times weaker than the $\nu_1 + \nu_3$ cannot be detected in the present experimental arrangement. At higher frequency, other band origins cannot be detected since our diode laser only covers the spectral region up to 6630 cm^{-1}. One relatively strong transition at 6622.954 cm^{-1}, line 776 from Ref. [14], (at the edge of the scan region of our diode laser!) is not assigned yet, but it is very unlikely that this transition belongs to one of the two identified bands.

As already mentioned in Section 1, many vibrational bands are expected in the 1.5 μm region: the $2\nu_1$, $2\nu_3$, $\nu_1 + \nu_3$, $\nu_1 + 2\nu_4$, $\nu_3 + 2\nu_4$, $4\nu_4$, $\nu_1 + 4\nu_2$, $4\nu_2 + \nu_3$, $4\nu_2 + 2\nu_4$, and the $8\nu_2$ bands, most of them having several $|l|$ components. Up to now, and including the present study, only three bands have been experimentally identified: two perpendicular bands at 6557 cm^{-1} (assigned as the $\nu_1 + 2\nu_4$ $|l| = 2$) and at 6609 cm^{-1}($\nu_1 + \nu_3$), and one parallel band at 6794 cm^{-1} ($2\nu_3$ $|l| = 0$ [14]).

However, since not all band origins in the 1.5 μm have been experimentally observed yet, the vibrational assignment of the observed bands is not straightforward. For example, the perpendicular band observed at 6557 cm^{-1}, which is in the previous section assigned to the $\nu_1 + 2\nu_4$ can as well be assigned to the $|l| = 1$ component of the $\nu_3 + 2\nu_4$. Following the procedure described by Mills [20], the effective ζ value (ζ_{eff}, defined as the value of ζ obtained by fitting the band as an $|l| = 1$ band) of the $|l| = 1$ component of the $\nu_3 + 2\nu_4$ state is $\zeta_{\text{eff}} = -\zeta_3 + 2\zeta_4$, while the ζ_{eff} of the $|l| = 2$ component of the $\nu_1 + 2\nu_4$ state (and of the $2\nu_4$ and $\nu_2 + 2\nu_4$ states) is $\zeta_{\text{eff}} = -2\zeta_4$. Since, $\zeta_3 \approx +0.05$ and $\zeta_4 \approx -0.23$, the ζ_{eff} of the $|l| = 1$ component of the $\nu_3 + 2\nu_4$ state is -0.51, while the ζ_{eff} of the $|l| = 2$ component of the $\nu_1 + 2\nu_4$ state is $+0.46$. Fitting the data set (from Table 1) to Eq. (1) with $|l| = 1$, taking into account the proper selection rules, results in the same rotational constants as listed in the last column of Table 2, but the value for ζ_{eff} is twice the value listed for ζ in Table 2 and has an opposite sign (thus $\zeta_{\text{eff}} = +0.40$). It is now evident that the $\nu_1 + 2\nu_4$ assignment is the right choice.

As an example of an alternative vibrational assignment, the perpendicular band at 6609 cm^{-1}, which is now assigned to the $\nu_1 + \nu_3$, can as well be assigned to the $|l| = 1$ component of the $\nu_3 + 2\nu_4$ (i.e., $l_3 = \pm 1$, $l_4 = 0$) which has the same ζ value as the $\nu_1 + \nu_3$ band. As a consequence, it cannot be ruled out that the vibrational assignment of the observed bands in the 1.5 μm region is incorrect. The rotational assignments (J and K labels) presented in this Letter, however, are still correct.

4. Conclusions

In order to be able to assign transitions from the vibrational ground state towards the lowest rotational levels of the $\nu_1 + \nu_3$ state, we have recorded the absorption spectrum of ammonia around 1.5 μm in a supersonic jet by using the sensitive CEA technique. Since the rotationally cold spectra of this band contain only a few fully resolved rotational transitions, an assignment could easily be made. A simple rotational analysis shows that the ΔB values are small, resulting in not well-resolved Q branches in the room temperature spectrum, which complicates its analysis.

Additionally, a new perpendicular band was identified in the jet spectra, which we assign to the

$|l| = 2$ component of the $\nu_1 + 2\nu_4$ band. The origin of this band is only 52 cm^{-1} red-shifted with respect to the origin of the $\nu_1 + \nu_3$ band.

Although a complete rovibrational analysis of the $\nu_1 + \nu_3$ and $\nu_1 + 2\nu_4$ bands is beyond the scope of present study, we hope that this study offers new starting-points for a full analysis in the near future.

Acknowledgements

This work is part of the research program of the 'Stichting voor Fundamenteel Onderzoek der Materie (FOM)', which is financially supported by the 'Nederlandse Organisatie voor Wetenschappelijk Onderzoek (NWO)', and receives direct support by NWO via PIONIER-Grant No. 030-66-89. This work is supported in part by the National Institute of Public Health and the Environment (RIVM).

References

[1] F.K. Tittel (Ed.), Appl. Phys. B 67 (1998) 273, Special Issue on Environmental Trace Gas Detection Using Laser Spectroscopy.
[2] M. Ohtsu, H. Kotani, H. Tagawa, Jpn J. Appl. Phys. 22 (1983) 1553.
[3] M. Fehér, P.A. Martin, A. Rohrbacher, A.M. Soliva, J.P. Maier, Appl. Optics 31 (1993) 2028.
[4] H. Ahlberg, S. Lundqvist, R. Tell, T. Andersson, Spectrosc. Eur. 6 (1994) 22.
[5] M. Fehér, Y. Jiang, J.P. Maier, A. Miklós, Appl. Optics 33 (1994) 1655.
[6] P. Cancio, C. Corsi, F.S. Pavone, R.U. Martinelli, R.J. Menna, Infrared Phys. Technol. 36 (1995) 987.
[7] A. Miklós, M. Fehér, Infrared Phys. Technol. 37 (1996) 21.
[8] R. Engeln, G. Berden, R. Peeters, G. Meijer, Rev. Sci. Instrum. 69 (1998) 3763.
[9] G. Modugno, C. Corsi, Infrared Phys. Technol. 40 (1999) 93.
[10] H.J. Unger, Phys. Rev. 43 (1933) 123.
[11] W.S. Benedict, E.K. Plyler, Can. J. Phys. 35 (1957) 1235.
[12] M. de Labachelerie, C. Latrasse, K. Diomandé, P. Kemssu, P. Cerez, IEEE Trans. Instrum. Measure. 40 (1991) 185.
[13] T. Wu, H. An, P. Jiang, Y. Fang, S. Tao, P. Ye, Optics Lett. 18 (1993) 729.
[14] L. Lundsberg-Nielsen, F. Hegelund, F.M. Nicolaisen, J. Mol. Spectrosc. 162 (1993) 230.
[15] Š. Urban, R. D'Cunha, K. Narahari Rao, D. Papoušek, Can. J. Phys. 62 (1984) 1775.
[16] G. Guelachvili, A.H. Abdullah, N. Tu, K. Narahari Rao, Š. Urban, D. Papoušek, J. Mol. Spectrosc. 133 (1989) 345.
[17] I. Kleiner, L.R. Brown, G. Tarrago, Q-L. Kou, N. Picqué, G. Guelachvili, V. Dana, J.-Y. Mandin, J. Mol. Spectrosc. 193 (1999) 46.
[18] N. Dam, C. Liedenbaum, S. Stolte, J. Reuss, Chem. Phys. Lett. 136 (1987) 73, and references therein.
[19] P.R. Bunker, P. Jensen, Molecular Symmetry and Spectroscopy, 2nd edn., NRC Research Press, Ottawa, 1998.
[20] I.M. Mills, Mol. Phys. 7 (1964) 549.
[21] Š. Urban, N. Tu, K. Narahari Rao, G. Guelachvili, J. Mol. Spectrosc. 133 (1989) 312.